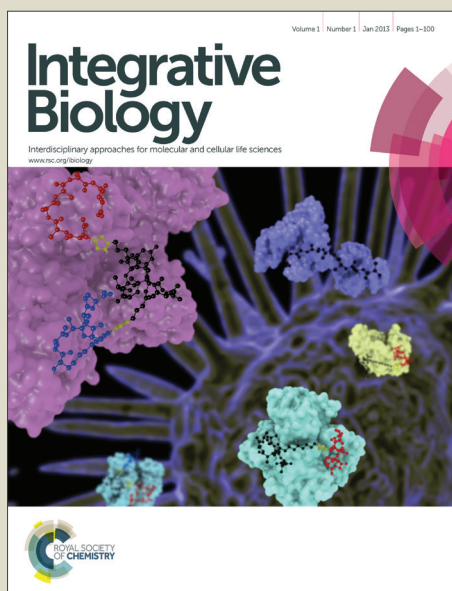


Integrative Biology

Accepted Manuscript



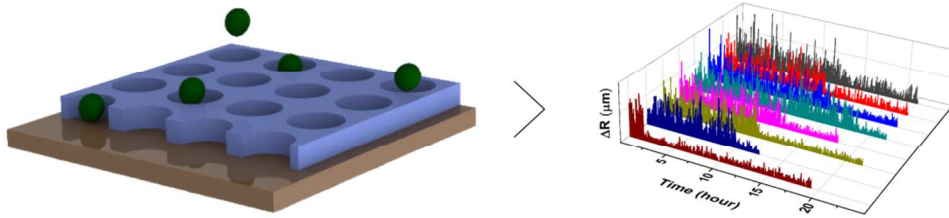
This is an *Accepted Manuscript*, which has been through the Royal Society of Chemistry peer review process and has been accepted for publication.

Accepted Manuscripts are published online shortly after acceptance, before technical editing, formatting and proof reading. Using this free service, authors can make their results available to the community, in citable form, before we publish the edited article. We will replace this *Accepted Manuscript* with the edited and formatted *Advance Article* as soon as it is available.

You can find more information about *Accepted Manuscripts* in the [Information for Authors](#).

Please note that technical editing may introduce minor changes to the text and/or graphics, which may alter content. The journal's standard [Terms & Conditions](#) and the [Ethical guidelines](#) still apply. In no event shall the Royal Society of Chemistry be held responsible for any errors or omissions in this *Accepted Manuscript* or any consequences arising from the use of any information it contains.

The analysis of Brownian motion is a sensitive and robust tool for a label-free high-throughput investigation of cell differentiation at the single-cell level.



Cite this: DOI: 10.1039/c0xx00000x

www.rsc.org/xxxxxx

ARTICLE TYPE

Marker-Free Detection of Progenitor Cell Differentiation by Analysis of Brownian Motion in Micro-Wells

Farzad Sekhavati,^a Max Endeke,^b Susanne Rappl,^a Anna-Kristina Marel,^a Timm Schroeder,^b and Joachim O. Rädler*^a

⁵ Received (in XXX, XXX) Xth XXXXXXXXX 20XX, Accepted Xth XXXXXXXXX 20XX
DOI: 10.1039/b000000x

The kinetics of stem and progenitor cell differentiation at the single-cell level provides essential clues to the complexity of the underlying decision-making circuits. In many hematopoietic progenitor cells, differentiation is accompanied by the expression of lineage-specific markers and by a transition from a non-adherent to an adherent state. Here, using the granulocyte-macrophage progenitor (GMP) as a model, we introduce a label-free approach that allows one to follow the course of this transition in hundreds of single cells in parallel. We trap single cells in patterned arrays of micro-wells and use phase-contrast time-lapse movies to distinguish non-adherent from adherent cells by an analysis of Brownian motion. This approach allowed us to observe the kinetics of induced differentiation of primary bone-marrow-derived GMPs into macrophages. The time lapse started 2 hours after addition of the cytokine M-CSF, and nearly 80% of the population had accomplished the transition within the first 20 h. The analysis of Brownian motion proved to be a sensitive and robust tool for monitoring the transition, and thus provides a high-throughput method for the study of cell differentiation at the single-cell level.

Introduction

Single-cell studies are increasingly being used in the biological and biophysical characterization of living cells. In contrast to population studies, which uncover only the average behavior of many cells, single-cell studies examine the underlying dynamics of the responses of individual cells to external triggers^{1,2}. Such experiments shed light on phenomena ranging from early signaling and responses at the level of protein synthesis to cell division and cell fate choices³. Single-cell analysis has also revealed phenotypic heterogeneity in isogenic populations^{4,5}. Stem cell fate decisions are prominent examples of heterogeneous system responses. The unique ability of stem cells to give rise to many kinds of differentiated cells makes them prime candidates for regenerative medicine. Thus, single-cell analysis of hematopoietic stem cell (HSC) decision-making promises to further our understanding of the regulatory factors underlying fate decisions, with potential impact on clinical medicine.

In recent years it has been recognized that, for single-cell analysis of stem cells in particular, there is a need for microscopy platforms that allow isolated cells to be cultured under conditions

that enable precise control over the mechanical and chemical properties of their micro-environment^{3,6}. This is because population studies have shown that the signaling molecules present⁷ and the mechanical properties of the environment^{8,9} can have a marked impact on stem-cell fates¹⁰. Microfluidic devices offer a highly accurate and flexible platform for this purpose, allowing both cell screening and micro-patterning^{11,12}. However, for most primary cells, and for non-adherent cells generally, isolation and tracking is difficult and time-consuming^{13,14}. Various microfluidic approaches have been developed to hold cells in place and facilitate long-term experiments. Active systems use e.g. hydrodynamic forces to create single-cell traps at the ends of microchannels¹⁵ or cell-sized, semi-circular barriers¹⁶, while passive systems such as micro-arrays of 3D micro-wells topologically trap the cells on the surface^{17,18}. In such devices, single-cell observations require the availability of fluorescent markers for the properties of interest. Fluorophore instability, bleaching, background noise and phototoxicity limit the application of fluorescence microscopy⁶. A label-free technique, which bypasses these limitations, is therefore highly desirable for time-lapse imaging of cells.

Here, we introduce a novel approach to follow the fate of isolated cells over time without the need to label them. The technique monitors the Brownian motion of single non-adherent cells to determine the timepoint at which they attach to the surface. Brownian motion of spherical objects is well understood and has been used as a sensitive probe for particle-substrate interaction in the case of microbeads¹⁹⁻²¹. We used image-based fluctuation analysis to resolve the heterogeneity of adherence transition times

^a Faculty of Physics and Center for NanoScience, Ludwig-Maximilians-University, Munich, Germany. Fax: +49-(0)89-2180-3182; Tel: +49-(0)89-2180-2438; E-mail: raedler@lmu.de

^b Department of Biosystems Science and Engineering (D-BSE), ETH Zurich, Mattenstrasse 26, 4058 Basel, Switzerland

† Electronic Supplementary Information (ESI) available: [details of any supplementary information available should be included here]. See DOI: 10.1039/b000000x/

at the single-cell level. Cells are confined to arrayed micro-wells and their motion is tracked over time using phase-contrast microscopy. As a proof of principle, we investigated the differentiation of granulocyte-macrophage progenitors in response to the cytokine M-CSF. During hematopoiesis, multipotent HSCs give rise to several lineage-restricted progenitors, which ultimately produce all the different mature blood-cell types²². Thus the bipotent granulocyte-macrophage progenitor (GMP) population gives rise to the monocyte/macrophage (M) and the granulocyte (G) lineages²³. In vitro, GMPs can be instructed to adopt the Ms or Gs fate by exposure to the cytokines macrophage colony-stimulating factor (M-CSF) or granulocyte colony-stimulating factor (G-CSF), respectively²⁴. Of these three types of cells, Ms are adherent while GMPs and Gs are non-adherent. We compare the timing of adherence of macrophages with the up-regulation of Lysozyme 2 (Lyz2), F4/80, and MacI, myeloid commitment/differentiation markers. We find that the adherence transition precedes the up-regulation of MacI, Lyz2 and F4/80 expression, hence following the general behavior observed by Rieger et al.²⁴ We demonstrate that the label-free technique is capable of robustly detecting the adherence transition, and discuss its potential for studying the kinetics of differentiation.

Results

Micro-structure fabrication

We fabricated micro-structured patterns on a tissue-culture plastic (TCP) substrate, which was then attached to the underside of a bottomless slide (I-Luer sticky slide; ibidi, Germany) to form the floor of a channel with walls 400 μm high. The pattern consists of an array of 3D micro-wells whose walls are 12 μm high. We tested different well diameters ranging from 15 to 50 μm and selected for the best single-cell coverage and maximum space for free diffusion. For GMPs (mean diameter 15 μm), micro-wells with a diameter of 35 μm were resulted in 90% viability and 60% single coverage. The micro-array pattern is fabricated from cell-repelling PEGDA polymer on a tissue culture plastic substrate²⁵. Each slide carries an array of 45 \times 750 micro-wells. Compared to conventional cell-culture flasks, the limited depth of the channel and the thinner layer of medium on top of the cells results in reduced background fluorescence, while still supplying enough nutrients for up to two days.

Cells in micro-wells

GMPs carrying an EGFP-tagged *Lyz2* gene (see Methods) were induced to differentiate into macrophages by adding M-CSF as previously described²⁴. Cells were pipetted into the channel and allowed to settle into the micro-well arrays (Fig. 1a). Three distinct states in the differentiation of GMPs into macrophages could be distinguished: a freely diffusive state subject to Brownian motion, a semi-adherent state, and a fully adherent state (Fig. 1b).

Non-adherent cells diffuse freely, ranging over the whole area of a micro-well. Semi-adherent cells attach to the surface and become immobile. Fully adherent cells spread out on the substrate and display active, crawling motion. Fig. 1c shows phase-contrast images of a representative cell going through each of the three states. For the purpose of differentiation detection, we

followed the positions of cells until just before division or until the transition to the fully adherent state. While the former breaks the symmetry in label-free detection, the latter is characteristic for a late stage of differentiation. The adherent state was observed to confirm that the cell had successfully reached the fully developed macrophage state, which could occur either in the same generation or after division.

Most of the cells in the non-adherent state ranged over the whole well area. In others, a tendency to remain close to the wall was observed. These latter cells show less difference in motion between the two states, but the switch to the adherent state is still distinguishable.

Time-lapse imaging

Time-lapse microscopy was performed using an inverted Axiovert 100M Zeiss microscope, taking advantage of the out-of-focus phase-contrast image, in which cells have bright centers. This accelerates cell recognition in image processing. Each sample is imaged at 3-min intervals for 24 h, producing a time-lapse sequence of cell motion (Fig. 2a). An interval of 3 min allows a cell of 15 μm diameter to be displaced by ~ 3 μm , which equals the ~ 5 pixel resolution in our microscopy setup.

Cell centers were tracked with an in-house ImageJ²⁶ plug-in. The software locates the micro-well array and automatically tracks the center of the cell until cell division or differentiation. For more details of the recognition algorithm see the Supplementary Information. Fig. 2b shows an example of one cell in a micro-well (red) and the cell contour (green) as detected by the software. Fig. 2c is the resulting trajectory of the center of the cell. All tracking data were processed simultaneously, decreasing the time required for analysis.

Confined Brownian motion in micro-wells

We used the mean square displacement (MSD) of cell position to characterize Brownian motion in confinement. As shown in Fig. 3, the plot of MSD vs time is linear at short time-scales, indicating free diffusion with a defined diffusion coefficient. In the case of confinement, as with cells in micro-wells, the MSD reaches a plateau value at large time-scales. As explained in more detail in the Supplementary Information, we used an explicit expression for the MSD for 2D diffusion in a circular confinement²⁷. The plateau value (P) in this case is given by $P = L^2/4$, where L denotes the clearance $L = d_{\text{well}} - d_{\text{cell}}$ between a cell with diameter d_{cell} and the wall of a micro-well with diameter d_{well} .

Fig. 3a shows the MSD for 10 individual GMPs exhibiting the characteristic shape of MSD for confined Brownian motion with the plateau value corresponding to the clearance. Three individual MSDs shown in color are compared to the theoretical expression (fits shown as lines). The cell diameters derived from the plateau of the MSD graphs (inset of Fig. 3a) and the images (values in Fig. 3b) are compatible with each other, as the out-of-focus image shrinks the apparent diameter of the cells, which accounts for the difference between the two values.

Transition point from non-adherent to adherent state

The transition from the non-adherent to the adherent state serves as a marker for the timepoint of GMP differentiation. To detect it, we monitored the Brownian displacement of cells between

successive frames ($\Delta R = |R_{i+1} - R_i|$) (Fig. 4a). This displacement depends on the diffusion coefficient and the physical constraints on motion. A non-adherent cell diffuses freely within the well, and thus shows a larger displacement per unit time than adherent cells, which are no longer subject to Brownian motion. Fig. 4a shows representative displacement records for 8 cells and the difference between the non-adherent state in the beginning and the adherent state at the end. For high-throughput parallel investigation of single cells, it is important that this transition point be automatically detectable.

The standard deviation of displacement over a rolling time-window of 5 frames, σ_5 , was used for automatic determination of the transition point. The standard deviation σ is an indicator of the degree of variation in the motion of a particle over the course of the time-window. A threshold value was chosen in such a way that σ_5 value drops below it after adherence. This value is manually chosen for one cell and used for the whole experiment. The time-point at which σ persistently drops below this threshold is taken as the transition point (red circle in Fig. 4b). Monitoring of the persistence of the transition to the low-motion regime permits one to distinguish the actual transition to adherence from short-term fluctuations in Brownian motion.

The cumulative sum (cusum) algorithm was used to confirm detection of the transition point. The cusum algorithm checks the global behavior of a system at each time-point and reports if there is a persistent regime change in the system^{28,29}. The algorithm yields transition points in agreement with the values obtained by the standard deviation approach. Both the cusum and standard deviation algorithm are described in detail in the SI.

Heterogeneity in time to adherence

Differentiation of GMPs shows stochastic dynamics^{30,24}, with each individual cell behaving differently (e.g. Fig. 4a). With the help of micro-well arrays we are able to capture and analyze the behavior of many cells in parallel. The transition point detection technique was used to identify the adherence of 789 cells in parallel. This represents a physical marker of differentiation of non-adherent GMPs into adherent macrophages. Fig. 5a shows the temporal distribution of single-cell adherence over a period of 30 h. All the cells were cultured under the same conditions. Monitoring began 4 h after addition of M-CSF to the progenitors. Around 40% of cells were adherent by the start of imaging. The number of adherence events then drops exponentially with time, and 80% of the cells have adhered to the TCP substrate prior to the first division.

The time course of differentiation was investigated via the onset of expression of the EGFP-tagged *lyz2* signal as well as the presence of *Mac1* and *F4/80* antibody markers. Fluorescent images were analyzed by setting fluorescence thresholds for each marker and counting of the number of *Mac1* and *F4/80* positive and *Lyz2*-GFP expressing cells respectively. Fig. 5b shows the percentage of adherent cells (black), together with the time course of *Mac1* positive (red), *Lyz2*-expressing (green), and *F4/80* positive (blue) cells over a period of 48 h. It can be clearly seen that *Lyz2* and *F4/80* expression follows the expression of *Mac1*. In contrast most adherence events occur slightly before *Mac1* expression. The kinetics of the increase of total adherence, however, is weaker than the steep increase of *Mac1* expression. For this reason we show the single cell correlations in more

detail. Fig. 5c shows the correlation between the adherence timepoints and the onset of the differentiation markers for all cells individually. Again there is a clear order in the expression of the differentiation markers, while their correlation with the adherence time points is weak. Adherence typically occurs before the onset of the differentiation markers (as seen by the fact that most data points fall above the dashed line indicating the isochronic events). However, there are individual cells that show *Mac1* or even *Lyz2* expression before the onset of adherence.

DISCUSSION

Our study demonstrates that arrays of micro-wells enable single-cell analysis of the transition from a non-adherent to an adherent state utilizing Brownian motion as reporter. GMPs exhibit heterogeneity in the timing of both the adhesion transition as well as differentiation at the single-cell level. Rieger et al.²⁴ previously observed by manual cell tracking and classification of adherence that the transition to the adherent state precedes up-regulation of the *Lyz2* marker protein in most cases. Our study reproduces these data quantitatively. In contrast to manual evaluation, our unsupervised approach allows for high temporal resolution and increased statistical accuracy of the adhesion time point. In addition we observe the temporal sequences of differentiation markers *Mac1*, *Lyz2* and *F4/80*. However, the correlation of these markers with the time-point of adherence is weak. Clearly adherence is an early indicator of differentiation. Yet, the statistics of adherence events does not seem to strictly depend on the stage of differentiation. Hence the molecular changes at the cell surface that allow for adhesion do not seem to be directly timed within the differentiation process. In future studies with surface functionalized micro-wells more refined adhesion studies can be carried out. Single-cell analysis of Brownian motion therefore provides a versatile label-free method for high-throughput detection of the adherence transition. In particular, in future work the micro-wells could be functionalized with specific antibodies in order to detect the expression of surface molecules and selectively modify adherence of cells to the micro-well surface. In this case, time-resolved studies on single cell surface protein expression could be carried out without the adverse effects of intense illumination for fluorescence imaging. The time interval chosen for phase-contrast imaging in our study was several minutes, but could be further reduced. Potentially, Brownian motion analysis is capable of resolving single molecule binding as shown by Wong et al. for latex particles³¹. Hence, single-cell adhesion arrays open up the possibility of single-surface-molecule studies on living cells for protein and membrane characterization^{32,33,31} and quantitative evaluation of numbers of adhesion sites. In principle, the only limitation on the observation time in our approach is the point of cell division. We believe that the highly parallel analysis of single cells by monitoring of Brownian motion is a powerful, high-throughput, label-free method, which is particularly promising for the time-resolved investigation of differentiation and the detection of changes in cell-surface properties of non-adherent cells.

Methods

Device fabrication

Our microfluidics devices are based on inert PEGDA (polyethyleneglycol diacrylate)³⁴. The template for the micro-well array is fabricated on a standard plastic tissue-culture (TCP) foils, which is attached to the underside of an I-Luer sticky slide (ibidi, Munich, Germany). The slide as supplied is patterned with a cut-out 400- μm deep channel that can be accessed from each end. The attached template thus serves as the floor of the channel. The fabrication process has been described previously²⁵. In short, the PDMS precursor is mixed with curing agent at a 10:1 (Sigma-Aldrich) ratio. The mixture is degassed for 15 min and then poured onto a patterned silicon wafer. After a subsequent degassing step for 15 min, PDMS is cured for ~ 3 h at 50°C in an oven. The PDMS mold is peeled from the wafer and cut along the structures to form an open network. PDMS and TCP substrate are exposed to argon plasma for 30 sec, then brought into contact with each other. A drop of PEGDA polymer (polymer solution containing 2% of photoinitiator 2-hydroxy-2-methylpropiophenone (v/v) (Sigma-Aldrich, Germany)) is placed at the open end of the PDMS mold. The empty space of the mold is filled with PEGDA by capillary force-induced flow. The polymer is then cured under UV light for 15 min. The PDMS mold is removed and the patterned PEGDA substrate is cured overnight at 50°C. The substrate is then sonicated in ethanol for 10 min, followed by a 10-min sonication in deionized water. Afterwards, it is blow-dried and attached to the ibidi I-Luer sticky slide and stored under sterile conditions.

Cell preparation

FACS purification of GMPs²³ from LysM:EGFP mice³⁵ was performed as described²⁴. Briefly, femora, tibiae, humeri, hip bones and vertebrae were dissected from 8- to 12-week-old mice, crushed in ice-cold 2% FCS/PBS, and cells were isolated by passage through a 40 μm filter (BD). All experiments were performed according to Swiss federal law and institutional guidelines of ETH Zuerich and approved by local animal ethics committee of Basel-Stadt (license number 2655).

For erythrocyte lysis, cells were resuspended in ACK buffer (Lonza) for 2 min. Cells were then stained with biotinylated antibodies against lineage-specific markers (B220, CD3e, CD19, CD41, CD11b, Gr-1, Ter119 (all eBioscience)) followed by incubation with streptavidin-coated magnetic beads (Roth). After magnetic depletion of labeled lineages, cells were stained with Streptavidin-APC-eFluor780, c-kit-PE-Cy7, CD34-eFluor660 (all eBioscience), Sca-1-Pacific Blue (Biolegend) and CD16/32-PE (BD) for at least 30 min on ice. Cell sorting was done on a FACS Aria III (Becton-Dickinson). Sorted GMPs were resuspended in SFEM (Stem Cell Technologies) containing 20 $\mu\text{g}/\text{ml}$ of M-CSF, 10 ng/ml F4/80 and 10 ng/ml MacI after markers. Time-lapse imaging was initiated 2 h after sorting and addition of cytokine, this time is necessary for transportation, seeding cells into micro-well arrays, and preparation of image acquisition setting.

The microscopy slide incubated at 37°C in an ibidi heating system chamber with 5% CO₂ and high humidity (ibidi, Munich, Germany). The chamber is mounted on an inverted microscope and a phase-contrast image is taken every 3 min and a fluorescent image every 3 h. Image acquisition is programmed to take a fluorescence picture of a subset of positions for each interval of phase-contrast imaging. Hence, we have fluorescent data at every

time-point.

Acknowledgements

We thank Christian Meggle for developing the image processing software. This work was funded by the Deutsche Forschungsgemeinschaft (DFG) via SFB1032, the Nanosystems Initiative Munich (NIM) Excellence Cluster, the International Doctorate Program in NanoBioTechnology (IDK-NBT), and the Graduate School of Quantitative Biosciences Munich (QBM).

References

- P. S. Hoppe, D. L. Coutu, and T. Schroeder, *Nat. Cell Biol.*, 2014, **16**, 919–927.
- T. Schroeder, *Nature*, 2008, **453**, 345–51.
- D. G. Spiller, C. D. Wood, D. A. Rand, and M. R. H. White, *Nature*, 2010, **465**, 736–45.
- M. a Walling and J. R. E. Shepard, *Chem. Soc. Rev.*, 2011, **40**, 4049–76.
- K. Chung, C. a Rivet, M. L. Kemp, and H. Lu, *Anal. Chem.*, 2011, **83**, 7044–52.
- S. Kobel and M. Lutolf, *Biotechniques*, 2010, **48**, ix–xxii.
- C. J. Flaim, D. Teng, S. Chien, and S. N. Bhatia, *Stem Cells Dev.*, 2008, **17**, 29–39.
- I. Kurth, K. Franke, T. Pompe, M. Bornhäuser, and C. Werner, *Integr. Biol.*, 2009, **1**, 427–34.
- J. M. Karp, J. Yeh, G. Eng, J. Fukuda, J. Blumling, K.-Y. Suh, J. Cheng, A. Mahdavi, J. Borenstein, R. Langer, and A. Khademhosseini, *Lab Chip*, 2007, **7**, 786–94.
- A. J. Engler, S. Sen, H. L. Sweeney, and D. E. Discher, *Cell*, 2006, **126**, 677–689.
- X. Mu, W. Zheng, J. Sun, W. Zhang, and X. Jiang, *Small*, 2013, **9**, 9–21.
- H. Yin and D. Marshall, *Curr. Opin. Biotechnol.*, 2012, **23**, 110–119.
- K. D. Kokkalis, D. Loeffler, and T. Schroeder, *Curr. Opin. Hematol.*, 2012, **19**, 243–249.
- T. Schroeder, *Nat. Methods*, 2011, **8**, S30–5.
- A. C. Rowat, J. C. Bird, J. J. Agresti, O. J. Rando, and D. A. Weitz, *Proc. Natl. Acad. Sci.*, 2009, **106**, 18149–54.
- S. L. Faley, M. Copland, D. Wlodkowic, W. Kolch, K. T. Seale, J. P. Wikswo, and J. M. Cooper, *Lab Chip*, 2009, **9**, 2659–64.
- H. Kim, R. E. Cohen, P. T. Hammond, and D. J. Irvine, *Adv. Funct. Mater.*, 2006, **16**, 1313–1323.
- V. Lecault, M. Vaninsberghe, S. Sekulovic, D. J. H. F. Knapp, S. Wohrer, W. Bowden, F. Viel, T. McLaughlin, A. Jarandehi, M. Miller, D. Falconnet, A. K. White, D. G. Kent, M. R. Copley, F. Taghipour, C. J. Eaves, R. K. Humphries, J. M. Piret, and C. L. Hansen, *Nat. Methods*, 2011, **8**, 581–6.
- D. C. Prieve and N. A. Frej, *Langmuir*, 1990, **6**, 396–403.
- J. Raedler and E. Sackmann, *Langmuir*, 1992, **8**, 848–853.
- V. Heinrich, W. P. Wong, K. Halvorsen, and E. Evans, *Langmuir*, 2008, **24**, 1194–203.
- S. H. Orkin and L. I. Zon, *Cell*, 2008, **132**, 631–644.
- K. Akashi, D. Traver, T. Miyamoto, and I. L. Weissman, *Nature*, 2000, **404**, 193–7.
- M. M. A. Rieger, P. P. S. Hoppe, B. B. M. Smejkal, A. C. Eitelhuber, and T. Schroeder, *Science (80-)*, 2009, **325**, 217–218.
- A.-K. Marel, S. Rappl, A. Piera Alberola, and J. O. Rädler, *Macromol. Biosci.*, 2013, **13**, 595–602.
- M. D. Abramoff, P. J. Magalhaes, and S. J. Ram, *Biophotonics Int.*, 2004, **11**, 36–42.
- T. Bickel, *Phys. A Stat. Mech. its Appl.*, 2007, **377**, 24–32.
- E. S. Page, *Biometrika*, 1954, **41**, 100–115.
- G. A. Barnard, *J. R. Stat. Soc. Ser. B Methodol.*, 1959, **21**, 239–271.
- D. Dingli, A. Traulsen, and J. M. Pacheco, *Cell Cycle*, 2007, **6**, 461–466.
- W. P. Wong, V. Heinrich, and E. Evans, *Mater. Res. Soc. Symp. Proceeding*, 2004, **790**, P5.1.1–P5.1.12.

-
32. A. Kusumi, Y. Sako, and M. Yamamoto, *Biophys. J.*, 1993, **65**, 2021–2040.
 33. A. Sonnleitner, G. J. Schütz, and T. Schmidt, *Biophys. J.*, 1999, **77**, 2638–2642.
 34. A. Khademhosseini, J. Yeh, S. Jon, G. Eng, K. Y. Suh, J. A. Burdick, and R. Langer, *Lab Chip*, 2004, **4**, 425–30.
 35. N. Faust, F. Varas, L. M. Kelly, S. Heck, and T. Graf, *Blood*, 2000, **96**, 719–26.

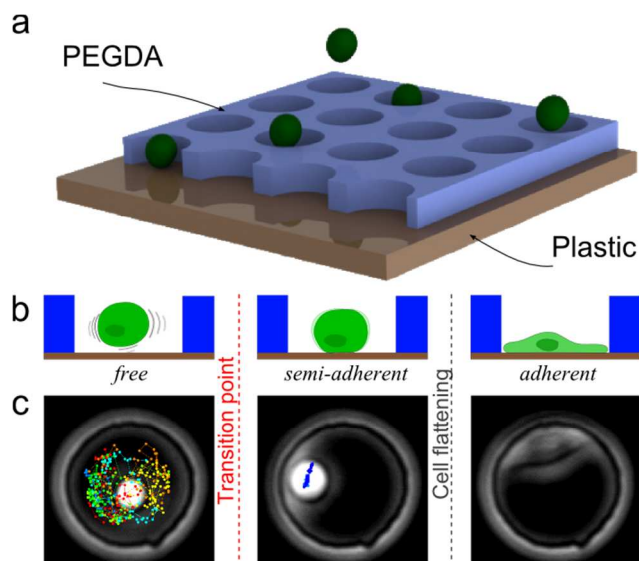


Fig. 1 a) Schematic view of cells settling into micro-wells under gravity. b) Schematic depiction of the three states of adherence: freely mobile, semi-adherent and adherent. c) Corresponding phase-contrast image of a non-adherent GMP which differentiates into an adherent macrophage. The dots indicate the position of the center of cell over a period of 24 h (elapsed time is coded in color from red to blue; see Fig. 2c). The transition point is the time at which the cell enters a semi-adherent state.

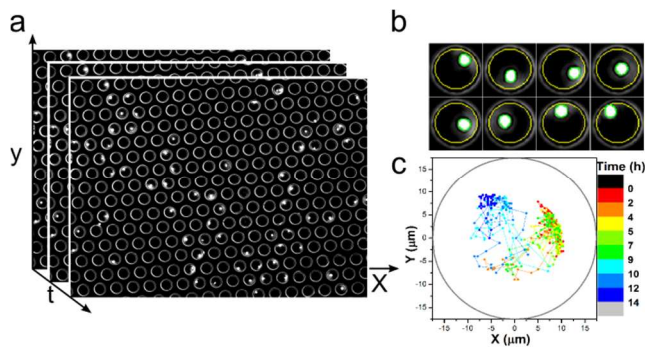


Fig. 2 a) Three frames from a time-lapse sequence of phase-contrast images of a single field at 10X magnification. The field contains ~250 wells and 50 single cells. b) Selected frames from a time-lapse sequence of phase-contrast images of a single well. Contours are detected automatically, the yellow contour indicates the micro-well and green contour indicates the center of the cell. c) Trajectory of the center of cell over a period of 14 h, (elapsed time coded in color as indicated), This cell adheres to the surface after around 12 h.

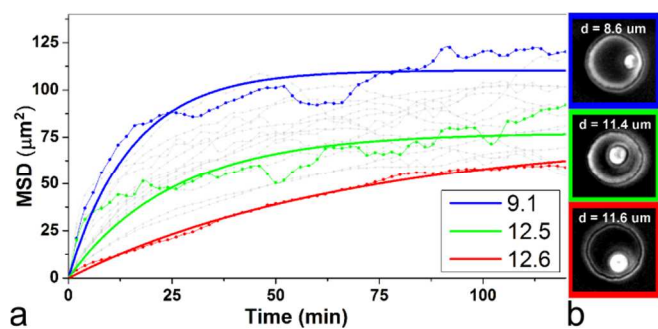


Fig. 3 a) Mean square displacement of cell center. The dots are experimental points and the solid line shows the fit from the explicit expression (See Supplementary Information). The different plateau values reflect differences in cell diameter. b) The corresponding phase contrast images of cells for solid lines are shown. Diameters calculated from fitted curves are shown in the inset and the diameter calculated from image calibration is shown on the corresponding image.

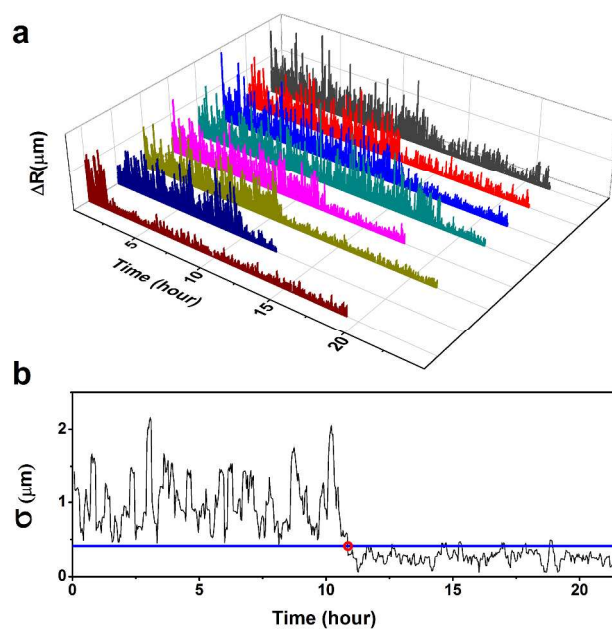


Fig. 4 a) Graph of cell displacement vs. time for a set of 8 single cells, showing how a non-adherent GMP cell differentiates into an adherent macrophage. b) Evolution of the local standard deviation σ over a rolling time window of 5 frames.

15

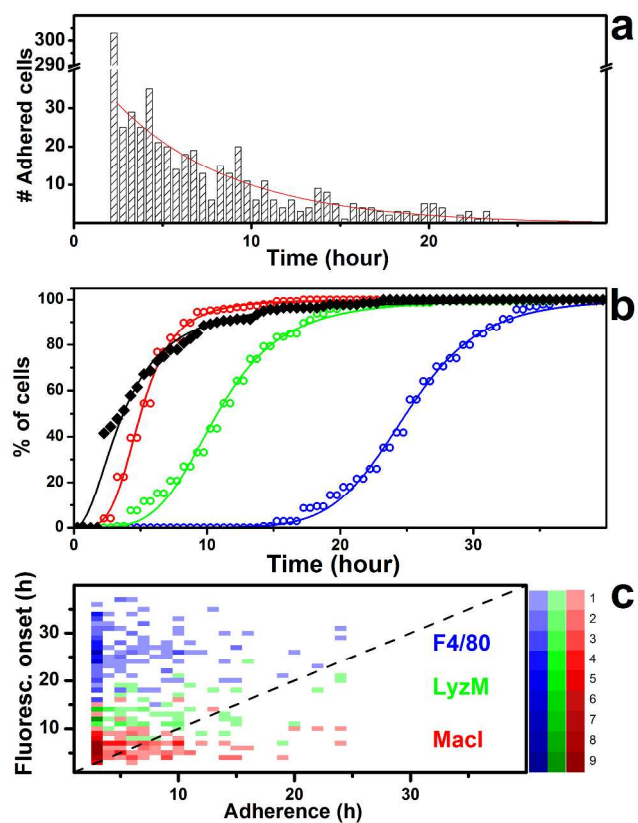


Fig. 5 a) Histogram of the number of adherence transitions in the time course of GMPs differentiation into macrophages (data are from 789 single cells), red line shows a first order exponential fit to the data. b) Percent of cells that adhered (black) and percent of cells that exhibited MacI (red), LyzM (green), and F4/80 (blue) fluorescent signal versus time. c) Correlation between the timepoint of cell adherence and the onset of the fluorescent signals. The dashed line indicates simultaneous events. The color intensity map indicates the number of cells.